The role of reconstructions in the identification of a wax/resin/gum tempera binder developed by Hermann Urban in 1901 and used by Cuno Amiet in 1902

The role of reconstructions in the identification of a wax/resin/gum tempera binder developed by Hermann Urban in 1901 and used by Cuno Amiet in 1902

Ester S.B. Ferreira, Karin Wyss, Violaine de Villemereuil, Karoline Beltinger, Federica Marone, Nadim C. Scherrer and Stefan Zumbühl

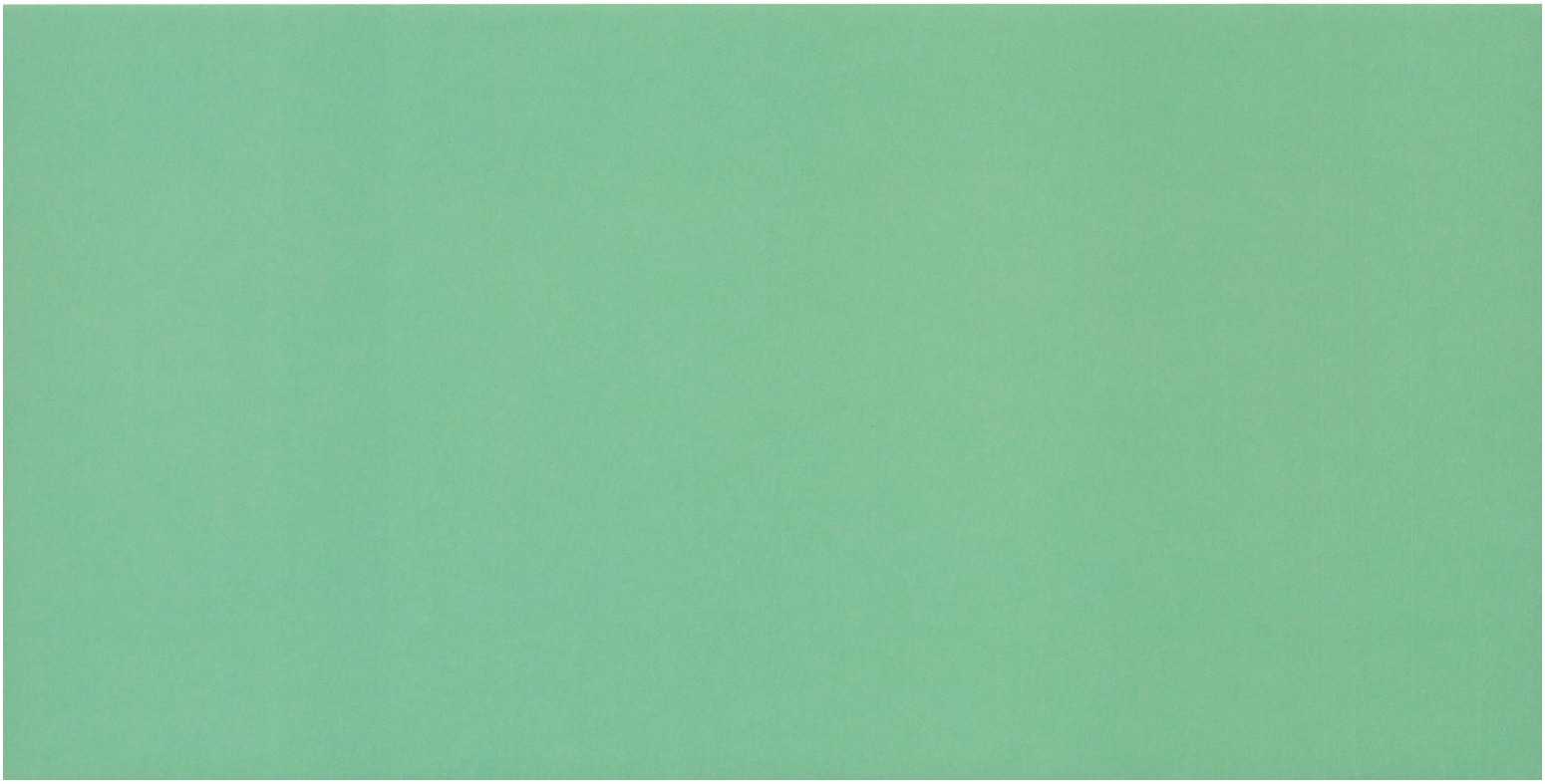

INTRODUCTION

During a comprehensive art historical and technical study of early paintings by the Swiss artist Cuno Amiet (1868–1961) conducted at the Swiss Institute for Art Research (SIK-ISEA) in Zurich, it became apparent that Amiet was interested in the expressive possibilities offered by diverse paint systems and application techniques. His paintings demonstrate a long-term involvement with extensive experimentation. Based on the study of written sources, such as Amiet's correspondence and notes, and on the results of our analyses of a number of his early paintings, we were able to establish that he used both commercial and home-made tempera paints of varied and complex compositions in addition to oils (Beltinger *et al.* 2015, pp. 51–71).

In the late 19th century, tempera paints gained in popularity as artists lost their trust in industrially produced oil paints. Tempera had a reputation as the favoured technique of the 'Old Masters' and was seen to be more resistant to age-induced alterations than oil paints. Its physical characteristics – it is fast drying and has a high luminosity – also made it appealing to artists. We assume that Amiet

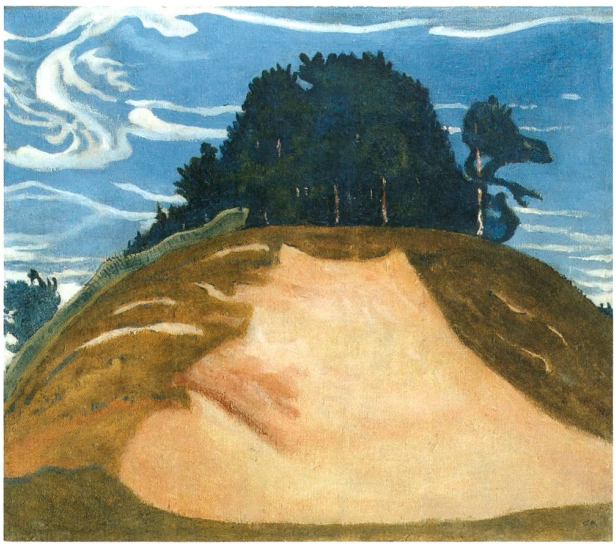

Fig. 2 Cuno Amiet, *Hügel (Hill)*, 1902, tempera on canvas support, 44 × 51 cm, Collection Pictet, Geneva.

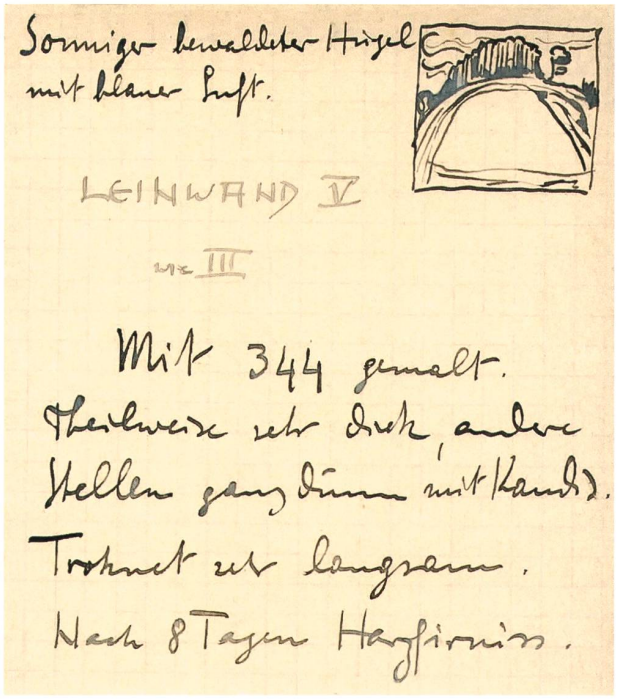

Fig. 1 Cuno Amiet, Notebook 1902–1905, 'Notes on the behaviour of paintings and studies created in diverse techniques ('*Aufzeichnungen über das Verhalten von in verschiedenen Techniken gemalten Bildern &. Studien*'), Oschwand (CH), Estate of Cuno Amiet. Detail of Amiet's entry concerning his painting *Hügel (Hill)* (see Fig. 2): 'Sunny wooded hill with blue sky. Canvas V / no. III / Painted with 344. / Partly thick, other / areas very thin with sugar. / Dries very slowly. / Resin varnish after 8 days' ('*Sonniger bewaldeter Hügel mit blauer Luft. / LEINWAND V / no III / Mit 344 gemalt. / Theilweise sehr dick, andere / Stellen ganz dünn mit Kandis. / Troknet sehr langsam. / Nach 8 Tagen Harzfirniss*').

first became aware of tempera between 1886 and 1992 during his time as a student in Munich and in Paris. We know that he made some initial, tentative use of tempera in the early or mid-1890s and began to employ it with regularity in 1899. During 1902 and 1903 he worked almost exclusively with tempera paints that he had prepared himself, which were based on recipes developed by a contemporary, the German artist Hermann Urban (1866–1948). Amiet possessed a compilation of recipes by Urban, dated 1901, which is preserved in his estate in Oschwand (Switzerland). The compilation encompasses 17 recipes – 13 tempera binders (provided with three-digit numbers), three

INGREDIENTS AND QUANTITIES FOR TEMPERA BINDER NO. 344						HOW TO PREPARE 'SENEGAL'	
344.			344.			SENEGAL	Senegal
SENEGAL	ccm	30	Senegal	ml	30	ARABI NATUREL	Gum arabic natural
KOPAIVAB	"	6	Copaiba balsam	"	6	KALT LÖSEN	dissolve cold
MASTIXFIR	"	24	Mastic varnish	"	24	1 Th. SE :	1 part senegal:
KANDIS	"	18	Rock sugar	"	18	1 Th. Aqua	1 part water
WACHS	Theelöffel	2	Wax	teaspoons	2	Durch Leinen drücken	Press through linen

HOW TO PREPARE 'ROCK SUGAR' AND 'MASTIC VARNISH', AND SOME ADVICE CONCERNING THE ADDITION OF WAX	
I. KANDISZUCKER 70 gr : 50 cc Aqua II. MASTIX 1 Th. : TERPENTIN 1 Th. III. WACHS IMMER FLIESSEND DER IM WARMWASSERBAD ERWÄRMTEN EMULSION ZULETZT BEIRÜHREN	I. Rock sugar 70 gr : 50 cc water II. Mastic 1 part: turpentine 1 part III. When mixing in the wax always add it as the last step, liquefied, to the emulsion which has been heated in a water bath.

HOW TO MAKE AN EMULSION	
EMULSIONS-HERSTELLUNG ZB. 317. MAN RÜHRT "SENEGAL" INNIG MIT COPAIVA ZUSAMMEN, JE EINZELN BERNSTEIN, MASTIX, KANDIS BEIRÜHREN. NIE ÜBER 5 cc DIESER FLÜSSIGKEITEN. REI[H]ENFOLGE EINHALTEN	Emulsion preparation e.g. 317. Mix 'senegal' well with copaiba balsam, add one by one amber, mastic [varnish], rock sugar [solution], never more than 5 ml of each of these liquids. Follow this sequence.

HOW TO GRIND AN EMULSION WITH PIGMENTS, AND SOME ADVICE ON PAINTING	
ANREIBE-RECEPTE 320. 344. 350.	Grinding instructions 320. 344. 350.
VERMISCHT MAN FARBE MIT EINEM DIESER RECEPTE BIS SIE BALLIG WIRD, REIBT KANDISLÖSUNG BEI, KANN MAN DIE FARBE ZU GEWOLLTER CONSISTENZ BRINGEN, FÜLLT SIE IN GUT VERSCHLIESSBARE "GLÄSER ODER TUBEN"	By mixing pigment with one of these recipes until it is thick, [and by] grinding rock sugar solution into it, one can bring the paint to the desired consistency. One fills 'glass jars or tubes' with them (*sic*) [that can be] well sealed
REIBT MAN EINEN GUT TROCKENEN FIRNISS- o. ÖLGRUND MIT DURCHSCHNITTENER ZWIEBEL AB, KANNMIT ALLEN EMULSIONEN DARAUF WEITERGEMALT WERDEN. "AUSGENOMMEN CASEINRECEPTE"	By rubbing off a thoroughly dry varnish or oil ground with a halved onion, [one] can continue to paint upon it with all emulsions. 'Except [for] casein recipes'
IN "DÜNNSTE" KOPAL, MASTIX, KOPAIVA, NUSSÖLEINREIBUNGEN KANN MIT ALLEN EMULSIONEN WEITER GEMALT WERDEN. "NICHT" MIT 249. 312	On 'the thinnest' impregnations [of] copal, mastic, copaiba, [or] walnut oil, [one] can continue to paint with all emulsions. 'Not' with 249. 312

Table 1 Excerpts from Hermann Urban's recipe compilation of 1901 from the estate of Cuno Amiet, Oschwand (CH): passages relevant to the preparation of Urban's tempera binder no. 344.

grounds and a fixative – and some instructions on their preparation and usage, all laid out on a single sheet of paper (Beltinger *et al.* 2015, pp. 58–71, 126–129).[1]

In this study special attention is given to a specific formulation in Urban's compilation, tempera binder no. 344, comprising a gum/resin/wax mixture (Table 1). According to a number of sources it was successfully employed by Amiet in 1902: a letter and a notebook entry of Amiet's from that year (Fig. 2) attest that he followed that precise formula to produce the paint that he used to create *Hügel* (*Hill*) (Fig. 1) (Beltinger *et al.* 2015, pp. 58–60).

The existence of the specific recipe for Urban's tempera binder no. 344 as well as the knowledge that Amiet employed this formulation in 1902 posed the challenge of how to formulate an analytical strategy that would allow us to confirm its use by means of microsamples taken from Amiet's

INGREDIENTS	PREPARATION	QUANTITY
Gum Senegal solution	1 part gum Senegal in 1 part cold water, filter	30 ccm
Copaiba balsam	No modification	6 ccm
Instruction: Mix the gum Senegal solution with copaiba balsam. Then take:		
Mastic varnish	1 part mastic in 1 part turpentine	24 ccm
Sugar solution	70 g rock sugar in 50 ml water	18 ccm
Instruction: Add the mastic varnish and sugar solution to the gum Senegal / copaiba balsam mixture slowly, no more than 5 ml at a time, to form an emulsion. Then take:		
Wax	Fluid (warm)	2 teaspoons
Instruction: Warm the emulsion in a water bath, then add warm, liquid wax.		

Table 2 Summary of Urban's instructions on the preparation of his tempera binder no. 344.

paintings. To this end, we reconstructed Urban's binder recipe and mixed it with lead white pigment to create a reference material.[2] In order to gain insight into the the ageing behaviour of the paint and to focus our analytical methods on the identification of its characteristic physical and chemical markers for the different components in its binder, the reconstructed paint was artificially aged and then chemically characterised with a number of analytical techniques. During the first part of this investigation, the location of the painting *Hügel* was unknown.

PREPARING THE RECONSTRUCTION

Urban's tempera binder no. 344 comprises the gum *Acacia senegal*, copaiba balsam, mastic varnish, unrefined sugar and wax. Urban indicates the precise quantities either in 'ccm' (cubic centimetres, i.e. millilitres) or in 'teaspoons', and also describes how to prepare the complex mixture (Tables 1 and 2).

INGREDIENTS	PREPARATION	SUPPLIER	QUANTITY
Gum Senegal solution	21.5 g Gum arabic 50 ml deionised water	Kremer	15,1 g (solution) (=15 ml)
Copaiba balsam	Copaiba balsam, 62100	Kremer	2,5 g (solution) (=3 ml)
Instruction: Combine gum arabic solution and copaiba balsam, using an electric stirrer → Mixture 1			
Mastic solution/ varnish	8.5 g Mastic, Chios, 60050 15 ml oil of turpentine, pure	Kremer	7,9 g (solution) (=12 ml)
IInstruction: Add 8.5 g mastic beads to 15 ml oil of turpentine. Allow to dissolve overnight, filter			
Sugar solution	70 g unrefined sugar 50 ml deionised water	Migros	7,8 g (solution) (=9 ml)
Instruction: Combine 7.8 g of the sugar solution and mastic varnish solution, using an electric stirrer → Mixture 2			
Combine mixtures 1 and 2, using an electric stirrer → Mixture 3			
Wax	Beeswax, bleached, 62210	Kremer	25 g molten wax (=1 teaspoon)
Instruction: Place the beeswax pellets in a beaker and melt them in a warm water bath at 75°C. Warm up mixture 3 in a water bath set at 60°C. Add liquid beeswax to warm mixture 3, using an electric stirrer to blend thoroughly.			

Table 3 Summary of the reconstruction process, carried out at SIK-ISEA Zurich in 2007, for Urban's tempera binder no. 344.

Reconstructing Urban's tempera binder no. 344

The materials and exact quantities used in the reconstruction and a detailed description of the individual steps are given in Table 3 and illustrated in Figs 3–6. Instead of employing *Acacia senegal* as indicated by Urban, commercial gum arabic was used. Gum arabic is a designation for a product made from any of a number of gums from the genus *Acacia*, of which *Acacia senegal* specifically is the most

important in commercial terms (Meer 1980; Mills and White 1994, p. 76). The gum arabic used for the reconstruction was purchased from Kremer Pigmente and most likely comprises *Acacia senegal* although the supplier could not confirm this with certainty.

Reconstructing the paint and preparing the paint strips

After some consideration, it was decided that grinding the pigment first in water and then combining the resulting paste with the tempera binder would have rendered the paint too thin. Subsequently, the pigment was ground directly with the tempera binder (Fig. 5) until a smooth, viscous paint was obtained. The working properties of the reconstructed paint were tested on a ground made from chalk and hide glue. The results were satisfactory: the paint was quite viscous, but easy to work. Applied thinly it was rather transparent, but its opacity improved with increasing thickness of the layer.

Paint strips of 100 µm thickness (Fig. 6) were produced with a Film Applicator Model 360 (Erichsen GmbH & Co, KG) on a silicon-coated Hostaphan® sheet RNT 36 (Kremer GmbH & Co, KG). The Hostaphan sheet was pre-cleaned with acetone.

Parameters for light ageing

The paint strips were light aged in a XENONTEST Alpha LM simulation chamber (Atlas GmbH, Germany) equipped with a 7-IR filter and a UV filter. The light source is selected to mimic the spectrum of daylight through glass with reduced IR radiation and a UV cutoff at 310 nm (DIN 54004). Total light exposure time was 1500 hours at 50 W/m2 and chamber conditions were held at RH = 50±1% and T = 40±2°C.

CHARACTERISATION OF THE CHEMICAL PROPERTIES OF THE RECONSTRUCTED PAINT

Prior to the reconstruction of Urban's tempera binder no. 344 as described above, samples of all of the individual materials used in the binder – mastic, gum arabic, rock sugar and beeswax – were chemically characterised by Fourier transform infrared spectroscopy (FTIR) and direct temperature resolved mass spectrometry (DTMS) to ascertain their purity and origin and to aid the interpretation of all later analyses. Next, samples from the naturally aged and light-aged reconstructed paint were also characterised by means of these two techniques. In order to gain two-dimensional spatially resolved information on the properties of the paint using light microscopy, scanning electron microscopy in backscattered electron mode (SEM-BSE), and attenuated total reflection-focal plane array-Fourier transform infrared spectroscopy (ATR-FPA-FTIR), cross-sections were made. In addition, a sample of the reconstructed paint was prepared to allow for the generation of three-dimensional information by means of synchrotron radiation X-ray tomographic microscopy (SRXTM). This approach, using multiple analytical techniques, was chosen with a view to facilitate cross-comparison of the depth and detail of information provided by each technique and to develop an analytical strategy that would maximise the information produced while minimising the amount of sample required from original works by Amiet.

FTIR analysis of naturally aged and light-aged samples

FTIR is a non-destructive analytical technique widely used in material studies. The energy of the vibrational, rotational and translational motions of a functional group within a molecule lies in the IR region. Since the energies of these motions depend on the composition and environment of the functional groups, the latter can be identified and interpreted as characteristic markers. Consequently, FTIR has become a very important diagnostic tool for material composition. Since the development of FTIR microscopes, the amounts of material required for analysis are minimal (µg range). The FTIR spectra and the detailed interpretation of the different absorption bands and spectral features of the individual materials comprising Urban's binder are presented in Appendix 2.

3

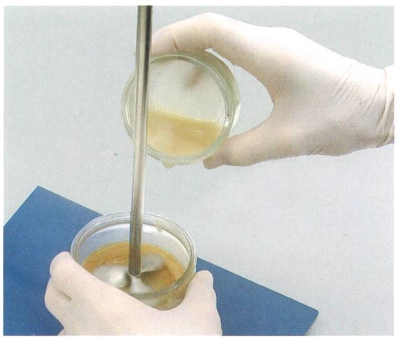

4

5

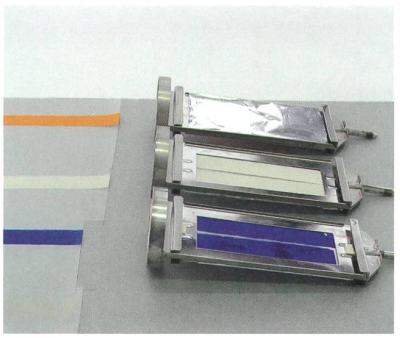

6

Fig. 3 Ingredients used in the reconstruction of Urban's tempera binder no. 344 (see Table 3).

Fig. 4 Reconstructing Urban's tempera binder no. 344: combining mixture 1 (gum arabic solution and copaiba balsam) and mixture 2 (mastic varnish and unrefined rock sugar solution) as described in Table 3. A homogeneous mixture was obtained with the help of an electric stirrer.

Fig. 5 Grinding the basic lead white pigment with the reconstruction of Urban's tempera binder no. 344.

Fig. 6 The reconstructed paint was applied on a Hostaphan film in 100 µm thick strips. The strips were cut to size and placed on sample holders in preparation for light ageing.

FTIR spectra from three samples from the naturally and light-aged strips of the reconstructed paint are shown in Fig. 7. The two upper spectra were collected from microsamples of the naturally aged paint strips kept at stable environmental conditions in the SIK-ISEA conservation studio, sheltered from light and analysed at a period of 3 and 65 months after execution. The lowermost spectrum was collected from a specimen of the same material that had instead been subjected to artificial light ageing for two months. The main FTIR bands are summarised in Fig. 7 and the band assignment can be found in Appendix 2. The FTIR spectra of all three samples are dominated by the contributions from beeswax, gum arabic and lead white pigment, with some minor absorption bands attributed to mastic. It should be noted that although FTIR spectroscopy allows for the identification of the major compound classes it does not permit the specific classification of ester wax, gum or resin type. Additionally the increased oxidation induced by the ageing of the mastic hinders the clear recognition of the presence of resin (as noted, only a few minor bands may be discerned).

Comparison of the spectrum of the naturally aged material with that of the light-aged paint shows that the carbonyl stretching band at 1706 cm^{-1}, characteristic of mastic, broadens with the increased oxidation induced by the light ageing; it cannot be clearly resolved in the spectrum of the light-aged sample. In addition, although unrefined sugar (present in relatively important amounts in the binder) gives a very distinct FTIR absorption pattern in crystalline form (see Appendix 2), it is not clearly identifiable in the FTIR spectrum of the reconstructed paint. This is due to the strong overlap with the absorption bands of gum arabic and probably a loss of crystallinity. Finally, minor and volatile compounds in the mixture, such as copaiba balsam and oil of turpentine, are present in quantities below the detection limit of FTIR within the bulk paint spectrum, even after the three-month ageing period. This allows us to conclude that FTIR analysis

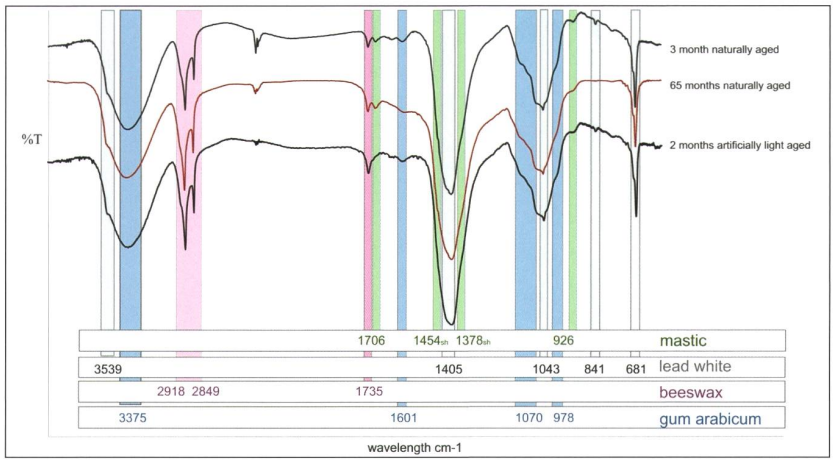

Fig. 7 FTIR spectra of the reconstructed paint after natural ageing and artificial light ageing. For detail peak assignments see Appendix 2, Figs 15–22 and 24–27.

of a sample from a historical painting that has been created with Urban's tempera binder no. 344 will, on its own, be inconclusive as it will not permit confirmation of the presence of either copaiba balsam or sugar, or allow identification of the exact resin, wax or gum types present.

DTMS analysis of naturally aged and light-aged samples

DTMS is a fast, minimally invasive technique that allows the recognition of the main components of a complex mixture. For example, the exact type of wax and triterpenoid resin can be characterised, sucrose can be identified and the presence of polysaccharide gums confirmed. The sample is suspended in a solvent and applied to a filament, which is inserted directly into the ion source when the solvent has evaporated. Progressive heating, from room temperature to pyrolysis, creates separate events from evaporation and desorption to pyrolysis of the different components or phases of the sample, over a period of two minutes. The gas phase ions are generated by low energy (16 eV) ion impact to minimise fragmentation. The spectrum of the individual events is then interpreted and compared with that of reference materials.

Again, prior to the analysis of the reconstructed paint, the individual components of Urban's tempera binder no. 344 were examined with DTMS. The spectra of the most important events are presented in Appendix 2.

The spectra of the DTMS analysis of samples of the reconstructed paint after 65 months of natural ageing are shown in Fig. 8. In event A (0.4–0.66 minutes) the main features of beeswax (m/z 256, 257, 368, 592, 620, 648, 676, 704), corresponding to palmitic and lignoceric acids, and the long-chain alcohol esters of palmitic acid dominate the spectrum. Also present are features of the mastic components and corresponding fragment ions (m/z 109, 203, 248, 424, 439 and 454).

The separation between events A and B is incomplete with a strong overlap. In event B the ions corresponding to the gum component (m/z 57, 60, 73, 85, 112, 114, 126) and sucrose (m/z 43, 57, 60, 73, 85, 97, 113, 115, 126, 127, 128, 144, 145, 149, 163) are the most important contributing species, although peaks corresponding to the wax and resin components may still be discerned despite the overlapping of events. Event C is dominated by the lead isotope ions (m/z 204, 206, 207, 208) from the lead white pigment.

The presence of copaiba balsam is harder to determine. Surprisingly, after 65 months of natural ageing, the peaks corresponding to the volatile sesquiterpene components of copaiba balsam (m/z 161, 189, 204) are still visible in event A. Very small peaks corresponding to the diterpenoid compounds from copaiba balsam (m/z 304 copalic

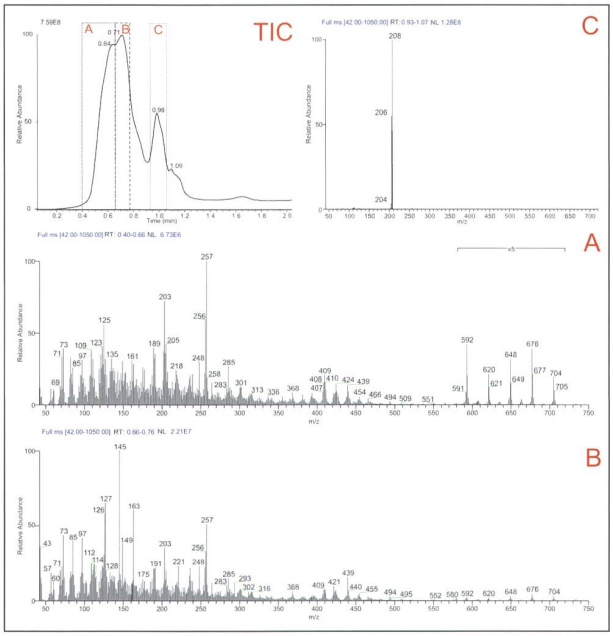

Fig. 8 DTMS analysis of the reconstructed paint, naturally aged for 65 months. The spectra are of the three most intense events.

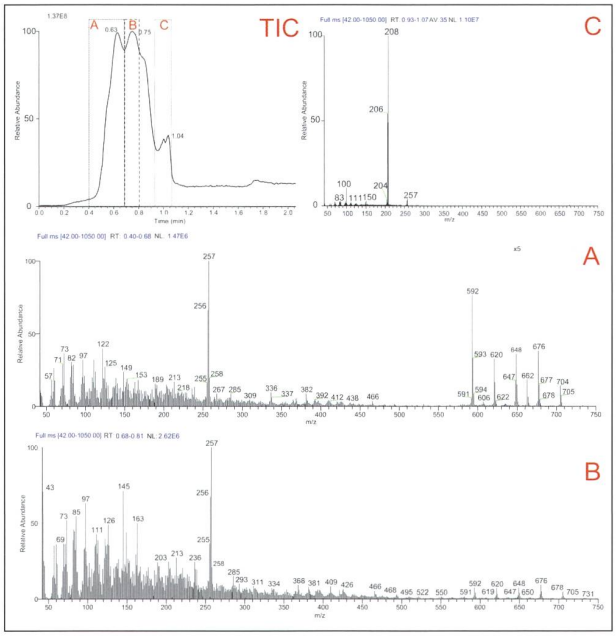

Fig. 9 DTMS analysis of the reconstructed paint, artificially light aged. The spectra are of the three most intense events.

acid) and the adulterant colophony (pine resin) (m/z 135, 285, 300 and 302 corresponding to quasimolecular ion and fragments of abietic, neoabietic and isopimaric acids) are also present. As these are at detection limit level, one would not expect to find significant amounts of copaiba balsam components in samples from paintings such as Amiet's, which are over 100 years old.

The spectra of the three most intense events of DTMS analyses of the light-aged reconstructed paint are shown in Fig. 9. Comparison of Figs 8 and 9 makes it possible to understand the effect light has on its composition. The most significant results of the intense light-ageing process are the loss of the mastic and copaiba balsam marker peaks and the partial loss of the fragments corresponding to the gum component. The beeswax and sucrose features are still clearly detectable in events A and B respectively. It can be concluded that the longer such paint ages, the more difficult identification of the most volatile and reactive components of the tempera binder will become.

Two-dimensional analytical imaging

A cross-section was prepared to allow for the spatially resolved analysis of a sample of the reconstructed paint. The subsequent investigations were designed to characterise the nature of the binder. A sample from the paint strip that had been naturally aged for 65 months was embedded in epoxy resin. More detail on the preparation methodology can be found in Appendix 1. The samples were investigated using light microscopy, SEM-BSE and ATR-FPA-FTIR imaging.

Images of the cross-section (Figs 10a and 10b) were taken with a light microscope in darkfield mode (DF) and with UV-induced visible fluorescence (UV LP430). Two areas indicated in red have a slightly duller appearance in DF mode but do not show fluorescent properties that are significantly distinct from the rest of the layer, thus suggesting only a minor difference in material composition.

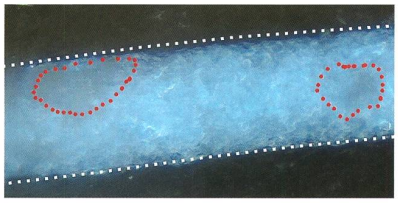

10a

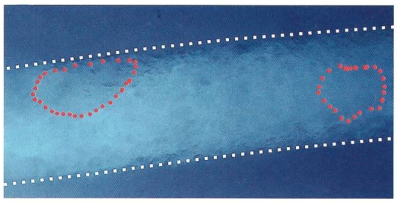

10b

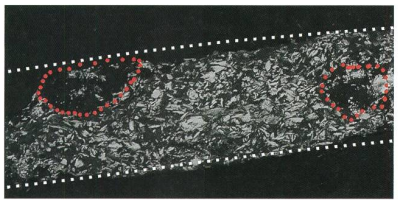

10c

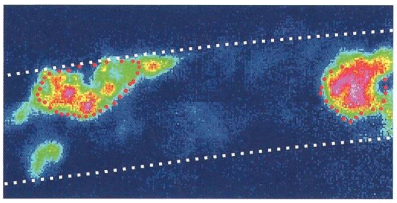

10d

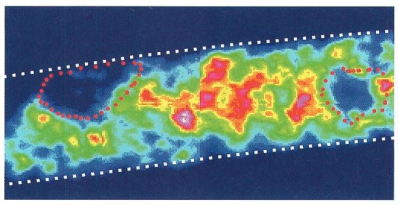

10e

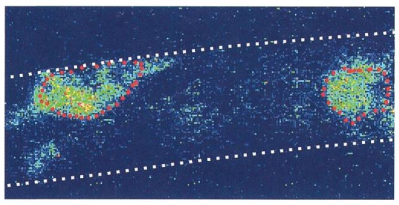

10f

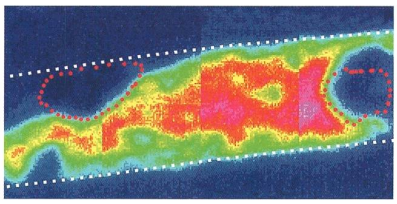

10g

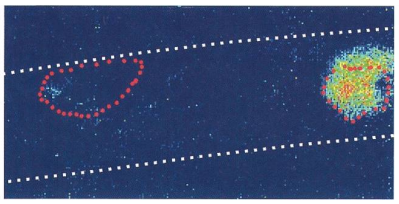

10h

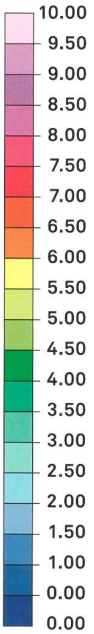

Figs 10a–10c Cross-section of the reconstructed paint, naturally aged for 65 months.

Fig. 10a Light microscopy image in darkfield mode.

Fig. 10b Light microscopy image in UV-induced visible fluorescence.

Fig. 10c Scanning electron microscopy image in backscattered electron mode.

Apolar regions (red dotted line) best described the absorbing regions of wax (Figs 10d, 10f, 10h).

Figs. 10d–10g ATR-FTIR-FPA (false colour) images of the cross-section.

Fig. 10d Absorption of C–H (2938–2894 cm^{-1}).

Fig. 10e Absorption of PbCO3 (1439–1306 cm^{-1}).

Fig. 10f Absorption of C=O (ester group) (1757–1726 cm^{-1}).

Fig. 10g Absorption of (C–O, C–O–H, C–O–H) polysaccharides (1096–973 cm^{-1}).

Fig. 10h Absorption of C=O resin carboxylic acids (1720–1693 cm^{-1}).

Examination of the same areas imaged by SEM-BSE (Fig. 10c) indicates a lower electronic density, suggesting a mainly organic composition. There is very little lead white pigment present in these these areas. SEM-BSE imaging also shows that the reconstructed paint has a heterogeneous morphology and composition.

While FTIR has long been established as a standard technique for the study of historic paint layers, the advent of ATR-FPA-FTIR has increased the analytical power of the technique. By providing two-dimensional spatial information at a resolution down to 1 µm, it is possible to localise and identify organic compounds *in situ* within microsamples. ATR-FPA-FTIR imaging is therefore particularly suited to the study of a multi-component system containing ingredients of different polarity but no emulsifier, such as Urban's wax/resin/gum tempera binder no. 344.

The capability of ATR-FPA-FTIR imaging is demonstrated in Figs 10d–10h, which reveal that the reconstructed paint consists of a heterogeneous two-phase system with large segregations caused by the differences in polarity of the individual phases. Apolar areas show strong absorption in the IR spectral regions attributed to C–H asymmetric stretching of the wax component (2938–2894 cm^{-1}, Fig. 10d), to carbonyl (C=O) stretching of the ester group of the wax (1757–1726 cm^{-1}, Fig. 10f) as well as to carbonyl (C=O) stretching of the ketones and primary carboxylic acids of the resinous components (1720–1693 cm^{-1}, Fig. 10h). The polar areas are characterised by strong absorption at regions attributed to the carbonate (CO_3^{-2}) asymmetric stretch in the lead white pigment (1439–1306 cm^{-1}, Fig. 10e), and to the C–O stretching of secondary alcohols and C–O–H bending, as well as to the asymmetric C–O–C stretch of the glycoside group of the polysaccharide gum (1096–973 cm^{-1}, Fig. 10g).

It is obvious that the lead white pigment is only bound in the polar polysaccharide gum phase. The wax and resinous components are distributed as separate inclusions. The polar and apolar phases are not clearly distinguishable by light microscopy, either in visible light or in UV-induced visible fluorescence mode, but can be satisfactorily visualised with SEM-BSE (Fig. 10c).

In conclusion, combined chemical imaging (i.e. SEM-BSE and ATR-FPA-FTIR) has revealed that Urban's tempera binder no. 344 is far from being a homogeneous system. Two main phases of different polarity can be distinguished within the morphology of the paint layers. The molecular information delivered by ATR-FPA-FTIR imaging has therefore proved to be informative with respect to the study of multi-component material mixtures such as tempera paint systems, by effectively revealing morphological information on compatibility and mixing at the micron scale.

Three-dimensional analytical imaging: SRXTM

The study of paint samples using SRXTM provides unique information on the three-dimensional distribution of phases of interest in an unmanipulated paint sample (Ferreira *et al.* 2009). With the goal of extending the ability to visualise the distribution of areas of lower electron density, such as the wax/resin agglomerates from a single cross-section to the entirety of a sample of the reconstructed paint, a particle of approximately 500 × 400 µm was analysed with SRXTM at the Tomographic Microscopy and Coherent Radiology Experiments (TOMCAT) beamline at the Paul Scherrer Institute in Villigen (Switzerland). The reconstructed data provided a cube of 8-bit greyscale images with a pixel size of 370 nm. The grey level of each phase depends on its absorption and scattering interaction with the X-ray beam and therefore on its composition. The wax/resin inclusions have a lower absorption resulting in a lower greyscale value, and segmentation of this phase allows the visualisation of the distribution of the inclusions in the paint layer (Fig. 11h). The inclusions measure on average 35–45 µm in diameter and are distributed throughout the entire sample. Orthogonal virtual sections (Figs 11d–11g) of the sample show that most of these inclusions are present in the uppermost regions of the paint layer. In the

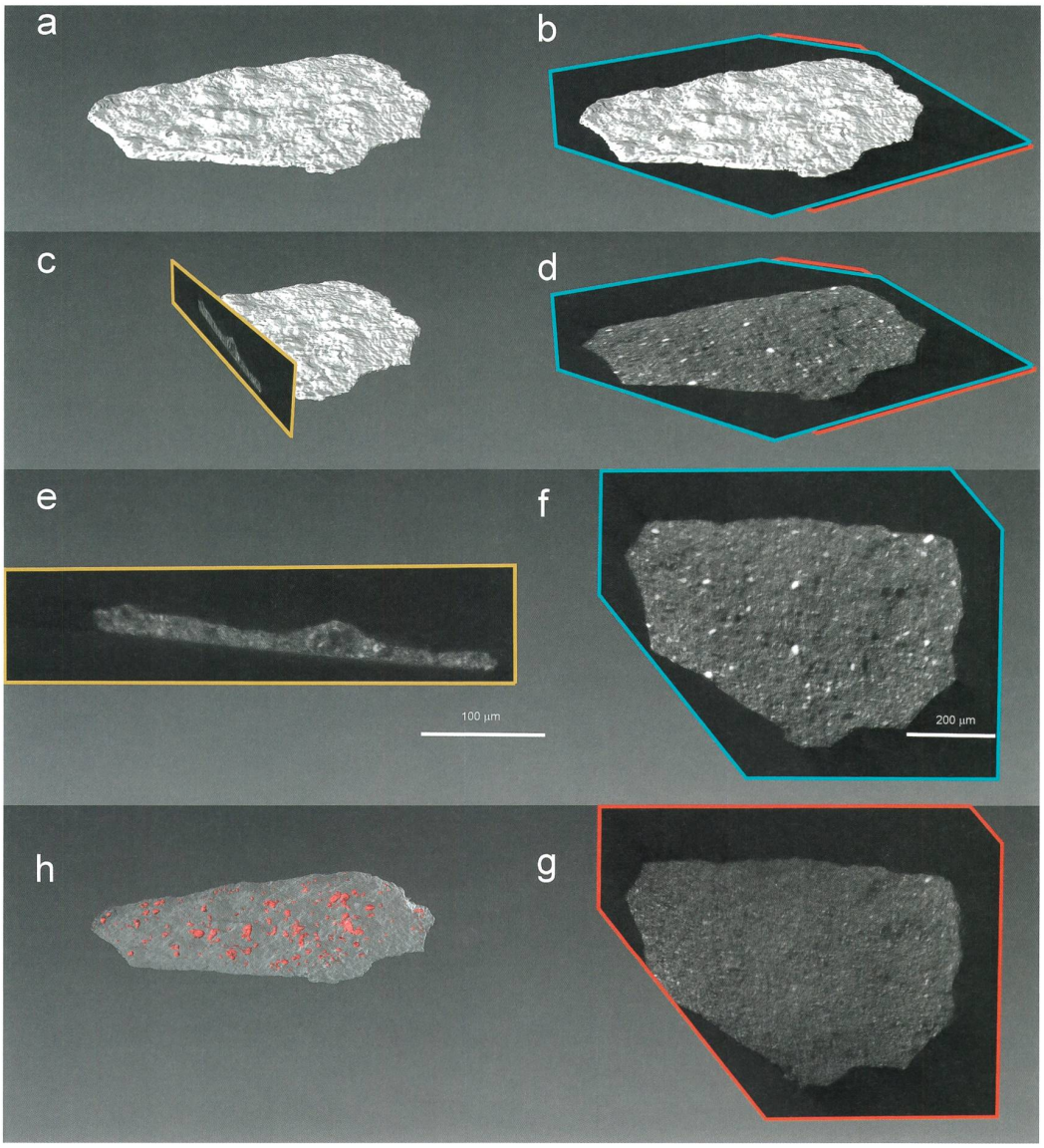

Figs 11a–11h SRXTM imaging of a sample of the reconstructed paint. The images clearly illustrate the heterogeneities within the paint.

Fig. 11a Outline of the sample analysed.

Fig. 11b Location of orthogonal slices shown in Figs 11d, 11f and 11g.

Fig. 11c Location of slice shown in Fig. 11e.

Fig. 11d Orthogonal slice as indicated in Fig. 11b.

Fig. 11e Slice as indicated in Fig. 11c.

Fig. 11f Orthogonal slice as indicated in Fig. 11b.

Fig. 11g Orthogonal slice as indicated in Fig. 11b.

Fig. 11h Distribution of wax/resin inclusions (red) within the paint layer.

lowest region of the paint layer (Fig. 11g), no inclusions are visible. This morphological feature, in combination with the analytical data, clearly indicates that the binder is to be identified as an emulsion.

AN ANALYTICAL STRATEGY FOR THE IDENTIFICATION OF THE USE OF URBAN'S TEMPERA BINDER NO. 344 IN CUNO AMIET'S PAINTINGS

A summary of the information obtained by each analytical technique tested with the reconstructed paint samples is given in Table 4. It can be concluded that in working with microsamples, comprising less than 50 µg of sample material, DTMS is the most effective technique for identification of the individual components. Prior to analysis with DTMS the sample can be examined by FTIR, as the latter is non-destructive, thus providing complementary multi-analytical evidence that supports the characterisation of the main compounds present.

The analytical imaging studies have shown that the type of emulsion represented by Urban's tempera binder no. 344 has a specific morphological feature – segregation of phases – that in itself could be suggestive of the presence of a tempera system. Additionally, the main components in each phase (an ester wax and polysaccharide gum) can be determined by ATR-FPA-FTIR analysis of a sample prepared as a cross-section.

ANALYSIS OF A PAINT SAMPLE FROM *HÜGEL (HILL)*, BY CUNO AMIET, 1902

In 2013 the location of the painting *Hügel* (*Hill*) (Fig. 2), which was described in Amiet's notes as having been created in 1902 with paint bound in Urban's tempera binder no. 344, was established. A small sample of white paint was collected from the painting for analysis. The sample was divided into two, one of which was analysed by bulk analysis (FTIR and DTMS) and the other by analytical imaging.

FTIR analysis

The pigment was identified as basic lead carbonate ('lead white'). The FTIR spectrum showed remarkable similarity to that of the naturally aged paint reconstruction: the major components were clearly resolved (Fig. 12).

ANALYTICAL METHOD	TYPE OF AGEING	DETECTION MASTIC	DETECTION BEESWAX	DETECTION GUM ARABIC	DETECTION SUGAR	DETECTION TURPENTINE	DETECTION COPAIBA BALSAM
FTIR	Natural	Resin	Ester wax	Gum	–	–	–
	Accelerated (light)	–	Ester wax	Gum	–	–	–
DTMS	Natural	Mastic	Beeswax	Gum	Sucrose	–	Copaiba balsam (weak)
	Accelerated (light)	–	Beeswax	Gum	Sucrose	–	–
ATR-FTIR-FPA	Natural	Resin (phase 1)	Beeswax (phase 1)	Gum (phase 2)	–	–	–

Table 4 Summary of the detectability of the individual components in Urban's tempera binder no. 344 by FTIR, DTMS and ATR-FTIR-FPA.

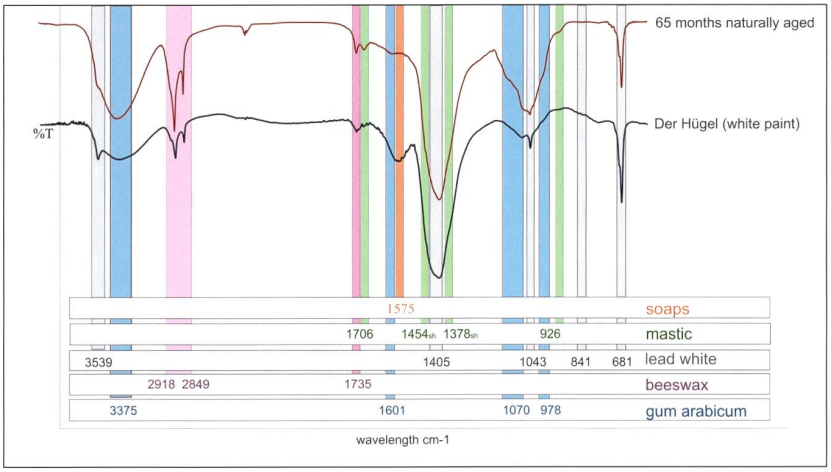

Fig. 12 FTIR spectra of a sample of white paint from the edge of *Hügel* (Fig. 2) and of the reconstructed paint.

Differences included the binder:pigment ratio, the broadening of the mastic C=O stretching band (1706 cm^{-1}) and the presence of metal soaps in the samples. The tempera paint prepared by Amiet and used to create *Hügel* has a much lower binder:pigment ratio, i.e. he used less binding medium and more pigment in formulating his paint, thereby probably initially producing quite a thick paste that he could easily have thinned with water to obtain the required level of fluidity.

Another significant difference related to the ageing process (both in terms of conditions and duration) is the presence of metal soaps and broadening of the mastic C=O band. The naturally aged sample of the reconstructed paint shows little evidence of strong oxidation of the mastic resin, which is to be expected since it was kept protected from direct light. The analysis of the light-aged sample (Fig. 7) shows that exposure to light induces oxidation, the effect of which is visible in the broadening of the C=O band.

The formation of metal soaps is a slow process at conditions of standard room temperature and humidity. The saponification of lipid-based paint systems can be recreated in artificial ageing conditions in an environment of high relative humidity in order to induce the hydrolysis of the carboxylic esters. However, as neither the samples that were naturally aged for 65 months nor those that underwent accelerated light ageing for three months were exposed to such humidity levels, one would not expect to find evidence for saponification in the paint reconstructions prepared for this study.

DTMS analysis

DTMS analysis of the white paint of *Hügel* (Fig. 13) shows a broad first band/peak, which under close inspection can be seen to result from overlapping of two, separate events. As demonstrated by the analysis of the reconstructed paint, in event A (0.4–0.70 minutes) the main features present are those of beeswax (m/z 256, 257, 368, 592, 620, 648, 676, 704) corresponding, as before, to the palmitic and lignoceric acid components as well as to the long-chain alcohol esters of palmitic acid. Also present, and consistent with the spectra generated from the reconstructed paint sample, are mastic components and the corresponding fragment ions (m/z 203, 248, 424, 439 and 454).

In event B the ions corresponding to the sucrose (m/z 43, 57, 60, 73, 85, 97, 113, 115, 126, 127, 128, 144, 145, 149, 163), and to a lesser extent the gum component (m/z 57, 60, 73, 85, 112, 114, 126), make the most important contribution to the resulting spectrum. The most intense peaks corresponding to the wax and resin components are still detectable in the spectrum of event B resulting from a partial overlap between events A and B. Event C is dominated

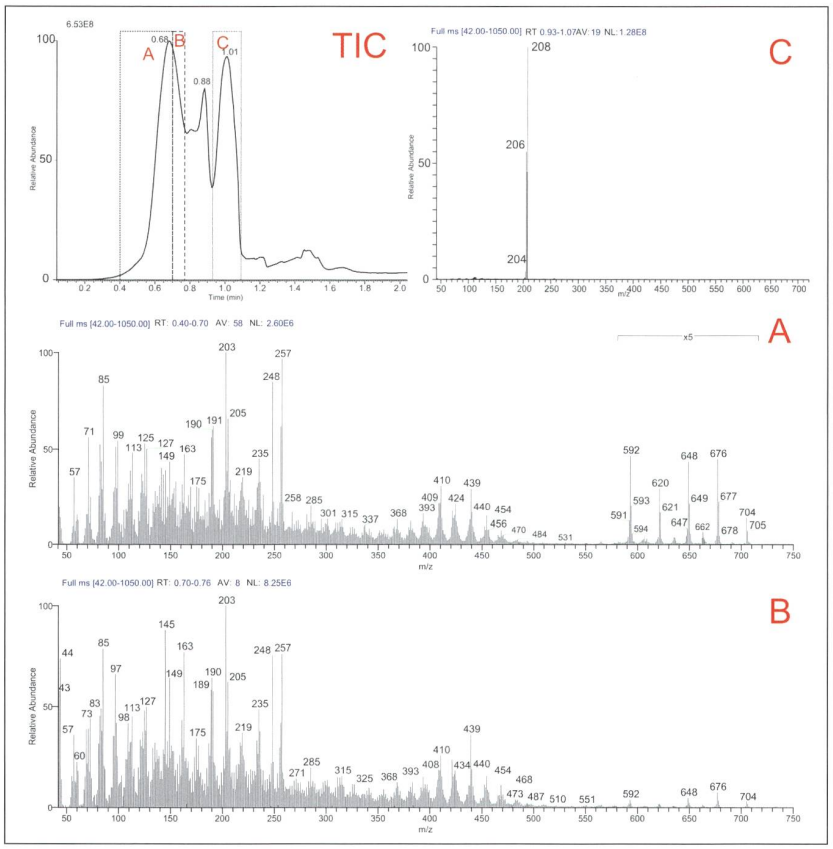

Fig. 13 DTMS spectrum of a sample of white paint from the edge of *Hügel* (Fig. 2).

by the ions characteristic of lead isotopes (m/z 204, 206, 207, 208) and in the total ion chromatogram (TIC) it can clearly be seen that the contribution from the pigment is more important in this sample than in that of the reconstructed paint. The presence of copaiba balsam could not be confirmed. DTMS identified the presence of a polysaccharide gum, sucrose, beeswax and mastic with a strong resemblance in profile to that of Urban's binder no. 344, further supporting FTIR evidence and contemporary written sources.

SRXTM and ATR-FPA-FTIR imaging

The second sample was analysed directly by SRXTM (without pre-testing by other means) and subsequently prepared as a cross-section for ATR-FPA-FTIR analysis. In the SRXTM analysis, spherical low X-ray attenuating areas of 20–30 µm diameter that are free of lead white pigment can be observed within the sample, similar to what was observed in the reconstructed paint (Fig. 14), which supported the identification of the binding medium as a type of tempera closely related, if not identical to, Urban's binder no. 344.

The analysis by means of ATR-FPA-FTIR was not entirely successful. Although good contact was achieved with the pigmented areas, the data were strongly dominated by the pigment signal. In the case of the low X-ray attenuating areas visualised by SRXTM, these were clearly exposed in the cross-section, but good contact was not achieved during ATR-FPA-FTIR and no conclusive signal was obtained. The reason for the lack of signal is unclear; however, it was observed that the lower density

phase seemed to be at slightly below surface level. During SRXTM the sample had been cooled under a flow of nitrogen (40°C) to avoid sample heating and material mobilisation. It is possible that the sample had not been adequately pre-cooled before the analysis, causing partial melting and subsequent mobility of the wax component. Significant movement of material could have lowered the quality and readability of the tomographic data considerably. Since the quality of the data was not substantially compromised, significant material movement can be excluded. Unfortunately no further sample material was available with which to attempt to clarify this issue.

CONCLUSION

The reconstruction and ageing of a tempera paint based on Hermann Urban's tempera binder no. 344 have permitted the development of an analytical strategy capable of identifying complex tempera mixtures with a minimal amount of sample material. Techniques such as gas chromatography-mass spectrometry (GC-MS), which employ multiple extraction and derivatisation steps in order to identify most classes of compounds, are powerful analytical tools and have been extremely successful in the analysis of complex mixtures of organic materials in wall painting binders and archaeological samples, as well as in easel paintings. These techniques, however, require larger amounts of sample material, in the 100s of µg range (Andreotti *et al.* 2006; Baumer *et al.* 2012). With the strategy developed herein, microsamples (in the 10 µg range) can be analysed to identify complex mixtures, such as this tempera binding system, with a good degree of confidence. The parallel paint reconstructions, which were made possible through information found in textual sources, combined with analyses of reference samples taken from the reconstructions, were extremely helpful in the interpretation of the data.

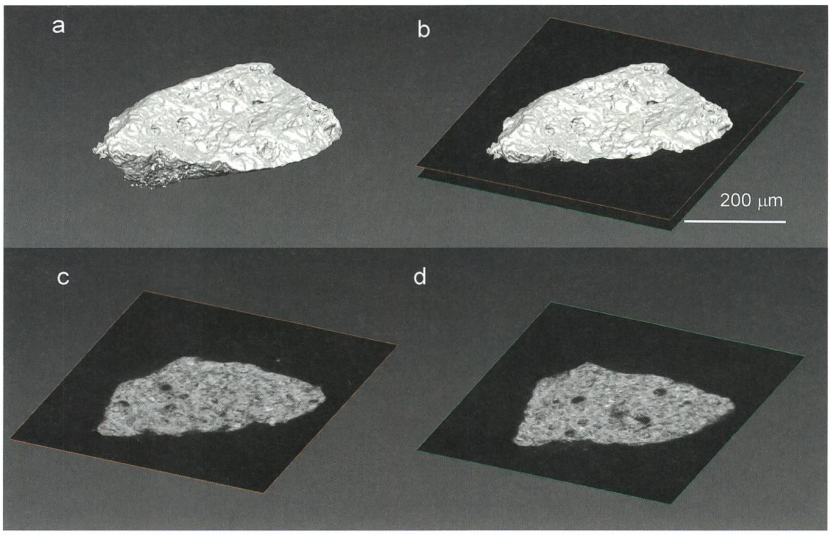

Fig. 14 SRXTM of a 300 × µm² sample showing areas of low X-ray attenuation within the sample.

APPENDIX 1: ANALYTICAL METHODS EMPLOYED

An analytical protocol combining various aspects – including analytical methodologies for the study of individual components in the reconstructed paint system as well as the resultant mixture, naturally aged and unaged – was developed. The aim was to improve the ability to characterise complex paint systems with minimal sampling.

FTIR

FTIR proved very useful in the non-destructive analysis of microsamples (5–10 µg) and in the characterisation of the main classes of compounds present. FTIR spectra were collected in a Perkin Elmer System 2000 spectrometer in transmission mode in a diamond cell, using a spectral range of 4000–580 cm^{-1} with a resolution of 4 cm^{-1} for 32 scans.

ATR-FPA-FTIR imaging

ATR-FPA-FTIR imaging was carried out in a Bruker Hyperion 3000 system with 64*64 FPA covering an area of 32 × 32 µm.

DTMS

DTMS was performed in a DSQII Thermo quadrupole instrument. The sample was suspended in methanol, applied to the rhenium filament and the solvent allowed to dry. The loaded filament was then resistively heated at a rate of 5 mA/s up to approximately 1000 mA. Ionisation was carried out in EI mode (pos), electron energy 16 eV, source temperature 250°C, with a scan range of 42–1050 amu. The data were analysed with Xcalibur software.

Cross-section

To prepare a cross-section, the sample was embedded in CEM 4000 light-curing resin and when set it was polished with the assistance of a MOPAS holder (JAAP Enterprise, Amsterdam, NL) on Micro-Mesh sheets up to grade 12000. Reconstructions for ATR-FPA-FTIR analysis were embedded in epoxy resin, Araldite 2020 (two-component XW396/397) and prepared as above.

Light microscopy

Light microscopy images of the prepared cross-section were taken on a Leitz DMRB microscope, equipped with Vis and UV (Osram HBO 103W/2) illumination and various filters for fluorescence imaging (Filter A = BP340-380, LP430; Filter I3 = BP450-490, LP515). A Jenoptik ProgRes Speed XT Core 3 camera with 2080 × 1542 pixel resolution is coupled to the system.

SEM-BSE

SEM-BSE density imaging of the embedded and uncoated sections was performed on a Zeiss EVO MA 10 tungsten VP-SEM, at a pressure of 30–40 Pa using a LM 5SBSD-detector at 10 kV acceleration voltage and 200 pA beam current.

SRXTM

For analysis by SRXTM the sample was attached to the sample holder with the aid of epoxy resin. The sample holder consists of a steel flat top rod, 32 mm in length and 500 µm wide at the sample level, which is fixed onto an aluminium base. Microtomographic scans were performed at the Swiss Light Source (SLS) in Villigen (Switzerland) at the TOMCAT beamline (Stampanoni *et al.* 2006). For each tomographic scan, 1170 projections over 180° were acquired (resulting in an angular step of 0.12°). For optimal contrast the energy was set to 34 keV and the exposure time per projection was 1700 ms. During measurement, the sample was cooled using a cryojet. Images were magnified using a 20× optical objective and digitised by CCD camera (PCO.2000) resulting in a pixel size of 0.33 µm. Tomographic reconstructions were computed using a highly optimised routine based on the Fourier transform method (Marone and Stampanoni 2012). The reconstructed data cube of images was processed and analysed in the commercial software AVIZO 8.1.

APPENDIX 2: FTIR AND DTMS REFERENCE SPECTRA OF THE INDIVIDUAL COMPONENTS IN HERMANN URBAN'S TEMPERA BINDER NO. 344

Ester S.B. Ferreira, Karin Wyss and Stefan Zumbühl

Mastic

Mastic is a triterpenoid resin that exudes from the tree of the species *Pistacia lentiscus* var. Chia DC (Anacardiaceae family) found on the island of Chios in Greece. Detailed chemical mass spectrometric characterisation has been published by van der Doelen (1999, pp. 30–31) and van den Brink (2001, p. 35). The assignments of FTIR bands in the spectrum (Fig. 15, Table 5) were based on published data (Bellamy 1975, pp. 8, 167, 176, 184; Shearer 1989, p. 377). In the DTMS analysis only the mass peaks of the most intense events were listed and assigned (Fig. 16, Table 6). The sample was acquired from Kremer Pigmente (catalogue no. 60050, mastic pearls from Chios).

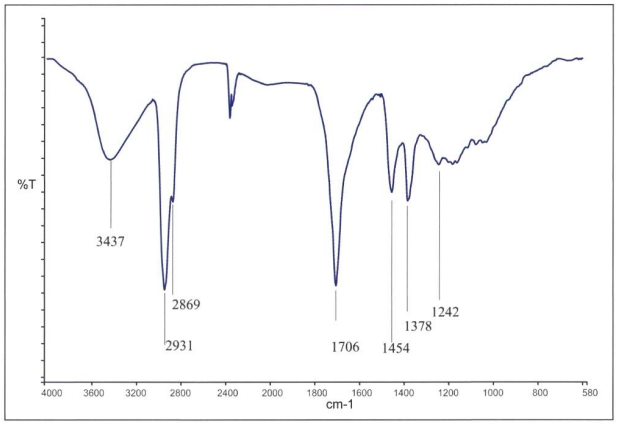

Fig. 15 FTIR spectrum of mastic.

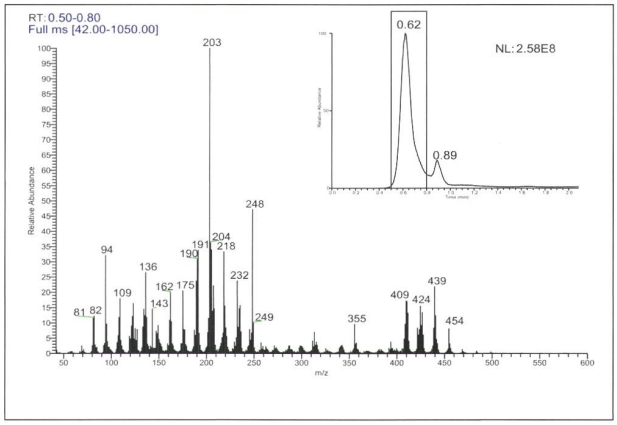

Fig. 16 DTMS spectrum of mastic.

FTIR band cm^{-1}	functional group
3437	O–H stretch (hydrogen bonded)
2931	C–H asymmetric stretching (CH_2 and CH_3)
2869	C–H symmetric stretching (CH_2 and CH_3)
1706	C=O stretching (ketones and carboxylic acids)
1454	C–H asymmetric deformation (CH_3 and CH_2 groups)
1378	C–H symmetric deformation (CH_3C and $(CH_3)_2C$)
1242	C–O stretch vibration of COOH (and other C–O containing functional groups)

Table 5 Assignments of FTIR bands in Fig. 15.

m/z	attribution	m/z	attribution	m/z	attribution
109	hydroxydam-marenone side chain fragment	**248**	fragment ion of oleanoic acid	**439**	isomastica-dienonic and masticadienonic acids (marker)
143	fragment ion ocotillone (ageing)	**355**	fragment hydroxydam-marenone	**454**	moronic acid
203	oleane or ursane skeleton fragment	**424**	hydroxydam-marenone		
232	oleane or ursane skeleton fragment	**426**	dammaradi-enol (3B hydroxy dammara-20, 24 diene)		

Table 6 Assignments of the most intense peaks of the DTMS spectrum in Fig. 16.

Beeswax

The main components of beeswax include hydrocarbons, esters and free acids, however the exact composition is dependent on the species of bee (Mills and White 1994, p. 49). Here, bleached beeswax from Kremer Pigmente (catalogue no 62210) was used. The bleaching process used on this material is not chemical; it was carried out with the aid of clarifying clay (Fuller's earth). The main distinction between our FTIR spectrum (Fig. 17, Table 7) and the FTIR spectrum of crude beeswax (Derrick *et al.* 1999, p. 184) is the absence of the O–H stretching band at 3450 cm^{-1}, indicating that the polar alcohol moieties were removed by the bleaching. The IR spectral interpretation was based on published data (Jones *et al.* 1952; Kühn 1960; Shearer 1989, pp. 203–204). The mass spectral interpretation of our DTMS analysis (Fig. 18, Table 8) was also based on existing literature (Languri and Boon 2005; Regert 2009).

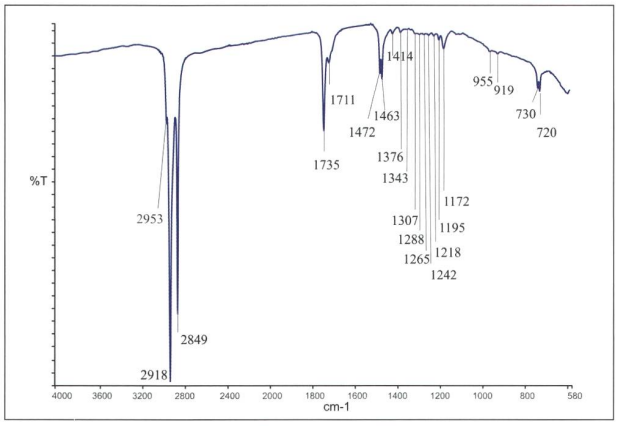

Fig. 17 FTIR spectrum of beeswax

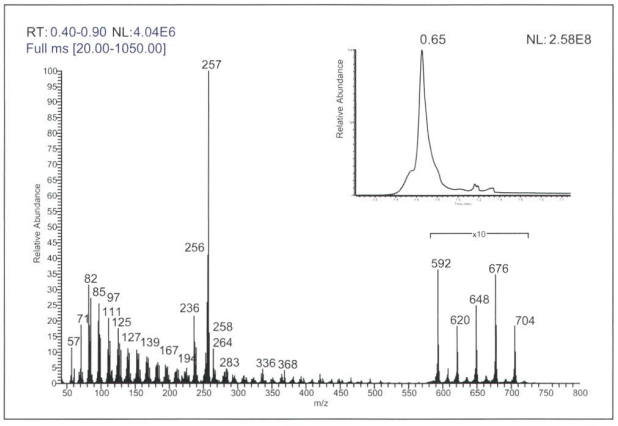

Fig. 18 DTMS spectrum of beeswax.

FTIR band cm^{-1}	functional group
2953	C–H asymmetric stretching (CH_3)
2918	C–H asymmetric stretching (CH_2)
2849	C–H symmetric stretching (CH_2)
1735	C=O stretching (ester group)
1711	C=O stretching (carboxylic acid group)
1472, 1463	CH_2 scissoring and deformation vibrations (crystal splitting)
1414	C–H deformation (ethyl group next to carboxylic acid)
1376	C–H deformation (methyl group)
1343	unassigned
1307-1171	C–H wagging and twisting vibrations (overtones)
1172	C–O–C asymmetric stretch (ester group)
955	unassigned
919	unassigned
730, 720	torsion chain vibration of long chain hydrocarbons (crystal splitting)

Table 7 Assignments of FTIR bands in Fig. 17.

m/z	attribution	m/z	attribution
256	palmitic acid	**620**	ester of hexacosanol (C26) with palmitic acid
257	palmitic acid fragment from wax esters	**648**	ester of octacosanol (C28) with palmitic acid
368	lignoceric fatty acid	**676**	ester of triacontanol (C30) with palmitic acid
592	ester of tetracosanol (C24) with palmitic acid	**704**	ester of dotriacontanol (C 32) with palmitic acid

Table 8 Assignments of the most intense peaks of the DTMS spectrum in Fig. 18.

Gum arabic

Gum arabic or gum arabicum is the exudate of the acacia tree; most commercially available gum arabic is derived from *Acacia senegal* (Meer 1980). It is a polymer composed of the hexose sugars rhamnose, galactose, glucuronic acid and galacturonic acid and the pentose sugar arabinose (Mills and White 1994, p. 77). The sample employed in this study was purchased from Kremer Pigmente (catalogue no. 63330) and most likely originates from *Acacia senegal* although this could not be confirmed by the supplier.

The IR spectral interpretation (Fig. 19, Table 9) was based on literature reports (Bellamy 1975, pp. 107, 135; Shearer 1989, pp. 385–386; Kačuráková and Mathlouthi 1996; Cui *et al.* 2007). The mass spectral interpretation (Fig. 20, Table 10) was extracted from published studies of the pyrolysis of gum arabic (Sjöberg and Pyysalo 1985; Räisänen *et al.* 2003) and from the DTMS of carbohydrates (Braadbaart 2004, p. 52 and references therein; Boon and Richter 2013). For the characterisation of oligo- and polysaccharides, chemical ionisation is more suitable (Lomax *et al.* 1991); however relevant characteristic fragment ions can be obtained in electron ionisation mode.

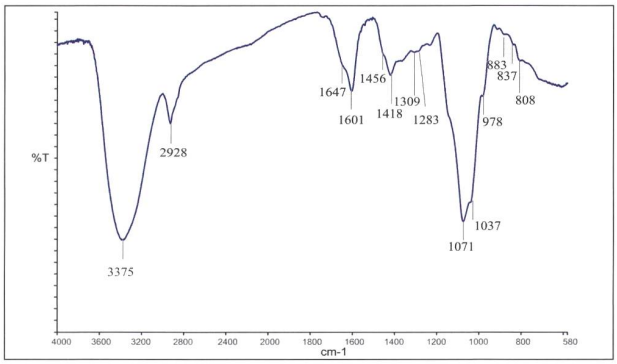

Fig. 19 FTIR spectrum of gum arabic.

FTIR band cm^{-1}	functional group
3375	O–H stretch vibration of hydroxyls (broadened by hydrogen bonds with water)
2928	broad C–H stretch symmetric and asymmetric (CH_2) (adjacent to primary alcohols $-CH_2-OH$)
1647-1601	O–H bending - (absorbed) water
1456	CH_2 deformation vibration (of primary alcohols $-CH_2-OH$)
1418, 1360	in-plane O-H deformation of primary and secondary alcohols (coupled with C–H wagging)
1309	C–H deformation vibration of the $R_2-(C-H)-OH$ group
1283	CH_2 twisted vibration (of primary alcohols $-CH_2-OH$) may be overlapped by OH deformation vibrations
1071-1037	C–O stretching of secondary alcohols and C–O–H bending asymmetric C–O–C stretch
978	symmetric C–O–C stretch
883	C–C–O stretch of secondary alcohols)
837	C–C–O stretch of secondary alcohols)
808	C–C–O, C–O–C symmetrical ring breathing vibration

Table 9 Assignments of FTIR bands in Fig. 19.

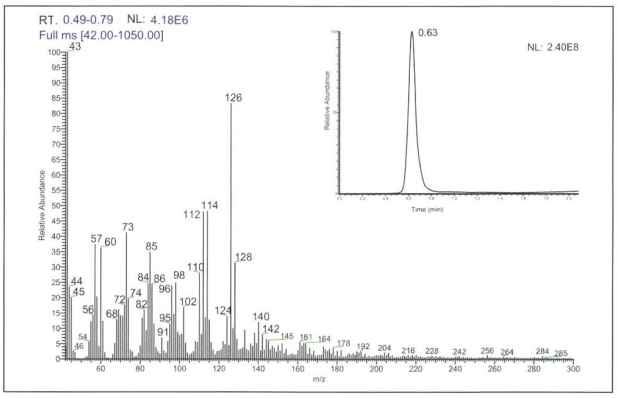

Fig. 20 DTMS spectrum of gum arabic.

m/z	attribution	m/z	attribution	m/z	attribution
57	Fragment ion of pyrolysis products of hexose sugars	**96**	pyrolysis hexose sugars 3-methyl-2-cyclopentenone furfural 2,4-hexadienal	**114**	pyrolysis pentose sugars
60	Fragment ion of pyrolysis products of hexose sugars	**98**	Fragment ion of pyrolysis products of hexose sugars	**126**	Fragment ion of anhydro-sugars 4-methyl-4-hepten-3-one 5-hydroxy-methyl-2 furaldehyde
73	Fragment ion of products of hexose sugars	**110**	2-furylmethyl-ketone	**128**	2-(1,2 dihydroxyethyl) furan
85	Fragment ion of pyrolysis products of hexose sugars	**112**	3-methyl-2-hydroxy-cyclopentenone		

Table 10 Assignments of the most intense mass peaks of the DTMS spectrum in Fig. 20.

Unrefined rock sugar

The sample of rock candy, or unrefined sugar, was of a modern commercial source and composed mainly of sucrose (verified by FTIR against an analytical grade sample from Sigma Aldrich). The attribution of individual absorption bands (Fig. 22, Table 11) was based on published data (Brizuela *et al.* 2012). Not all bands were labelled (more detailed description can be found in Brizuela *et al.* 2012). The labelled chemical structure of sucrose is shown in Fig. 21. The DTMS spectrum from rock sugar (Fig. 23, Table 12) contains a mixture of fragmentation ions and ionised pyrolysis products of sucrose (Johnson *et al.* 1969; Paine III *et al.* 2008; Paine III *et al.* 2008a; Paine III *et al.* 2008b).

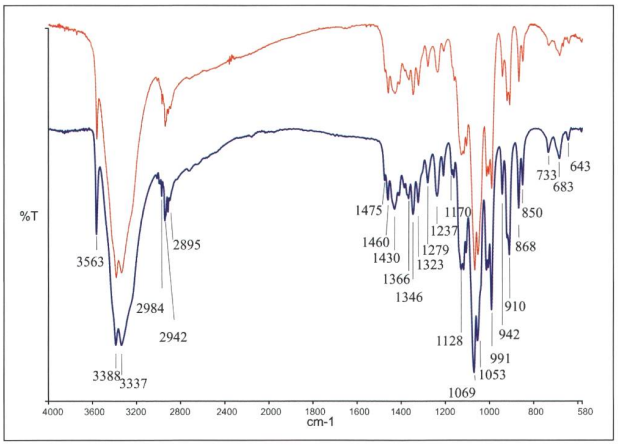

Fig. 22 FTIR spectrum of unrefined rock sugar.

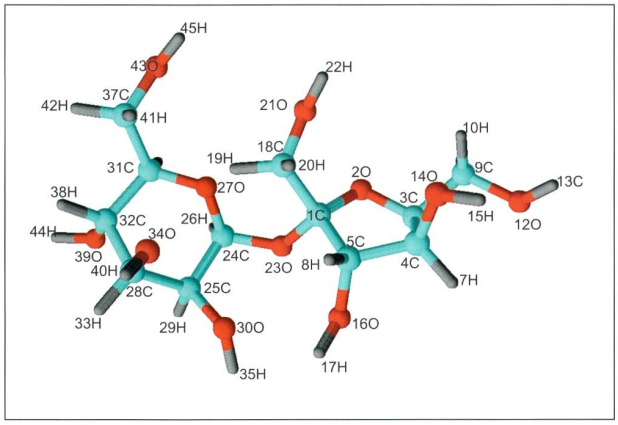

Fig. 21 Labelled chemical structure of sucrose (green: carbon; red: oxygen; grey: hydrogen).

FTIR band cm^{-1}	functional group
3563	O–H stretching (O14–H15, O21–H22, O43–H45)
3388	O–H stretching (O12–H13)
3337	O–H stretching (O30–H35)
2984	C–H asymmetric stretching (CH_2)
2942	C–H symmetric stretching (CH_2)
2895	C–H stretching
1475	CH_2 scissoring
1460	CH_2 scissoring
1430	CH_2 wagging, C-H in plane rocking (C28–H33 and C25–H29)
1366	C–H in plane rocking (C31–H36)
1346	CH_2 in plane rocking, C–H in plane rocking (C5–H8)
1323	C–H in plane rocking (C4–H7)
1279	C–H in plane rocking (C3–H6), CH_2 in plane rocking
1237	O–H deformation (O14–H15), O30–H35, O21–H22)
1170	C–C stretching (C1–C18)
1128	C–O stretching(C5–O16)
1069	C–C stretching (C37–C31), C–O stretching (C9–O21, C18–O21)
1053	C–O stretching (C9–O12, C18–O21)
991	C–O stretching (C28–O34, C1–O23)
942	C–C stretching (C23–C32)
910	twist CH_2
868	O–C–C scissoring (23–C24–27)
850	twist CH_2
733	C–O stretching (C31–O27), βR1 (ring deformation)
683	O–C–C scissoring (O34–C28–C32), O–C–O scissoring (O23–C24–O27)
643	βR1 ring deformation

Table 11 Assignments of FTIR bands in Fig. 21.

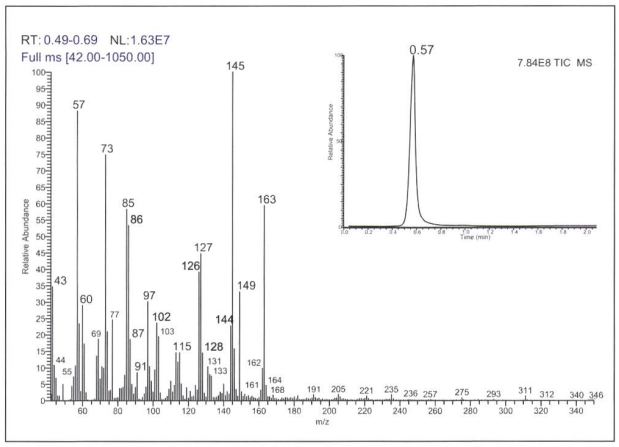

Fig. 23 DTMS spectrum of unrefined rock sugar.

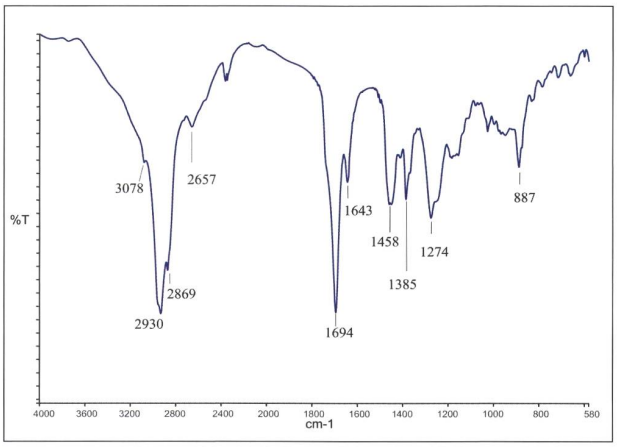

Fig. 24 FTIR spectrum of 'copaiva balsam'.

m/z	attribution	m/z	attribution
43	fragment ion sucrose	**58**	pyrolysis sucrose: propan-2-one, acetone, propanal
57	fragment ion sucrose	**68**	pyrolysis sucrose: furan
60	fragment ion sucrose	**74**	pyrolysis sucrose: 1 hydroxypro pan-2-one
73	fragment ion sucrose	**86**	pyrolysis sucrose: 1 hydroxy-but-3-en-2-one
85	fragment ion sucrose	**98**	pyrolysis sucrose: 5 methyl dihy drofuran-2-one, 2 hydroxyl methylfuran
97	fragment ion sucrose	**102**	pyrolysis sucrose: 4 hydroxydihydrofuran-3-one
103	fragment ion sucrose	**110**	pyrolysis sucrose: 5 methyl furfural
113	fragment ion sucrose	**126**	Fragment ion sucrose pyrolysis sucrose: 5 hydroxymethyl-2 furaldehyde, 2-furyl-hydroxy methyl ketone, methylfuran-3-carboxylate
115	fragment ion sucrose	**128**	pyrolysis sucrose: 2 (1,2 dihydroxyethyl furan
127	fragment ion sucrose	**144**	pyrolysis sucrose
145	fragment ion sucrose	**149**	fragment ion sucrose
163	fragment ion sucrose		

Table 12 Assignments of the most intense peaks of the DTMS spectrum in Fig. 22.

FTIR band cm^{-1}	functional group
3078	C–H asymmetric stretching of the methylene group =CH2 (vinylidene) and aromatic rings =C–H
2930	C–H asymmetric stretching (CH2 and CH3)
2869	C–H symmetric stretching (CH2 and CH3)
2657	O–H stretching (carboxylic acid hydrogen bonded)
1694	C=O stretching (several overlapping carboxylic acids providing a broad signal)
1643	Mainly C=C stretching of methylene group (vinylidene)
1458	C–H asymmetric deformation (CH3 and CH2 groups)
1385	C–H symmetric deformation (CH3)
1274	C–O stretch vibration of COOH
887	>C=C stretching of methylene group (vinylidene)

Table 13 Assignments of FTIR bands in Fig. 24.

Copaiba balsam

Copaiba balsam is a diterpenoid resin of natural origin produced by trees of the genus *Copaifera*. The material used here as reference was acquired from Kremer Pigmente (catalogue no. 62100). The analysis by GC-MS according to a procedure described in the literature (van der Werf *et al.* 2000) showed the presence of the copaiba sesqueterpenes (copaene, caryophyllene) and diterpenoids (karuran-16–18-oic acid, copalic acid, acetoxy-copaiferic acid, hardwickiic acid, acetoxy hardwickiic acid), but also other diterpenoids as abietic acid, neoabietic acid, pimaric acid, sandopimaric acid, isopimaric acid and palustric acid, indicating the presence of pine colophony (van den Berg *et al.* 2000; van der Werf *et al.* 2000). DTMS peak assignment (Fig. 25, Table 14) was based on known fragmentation patterns of the main chemical components of copaiba balsam (van der Werf *et al.* 2000) and pine colophony (van den Berg *et al.* 2000). FTIR band attribution (Fig. 24, Table 13) was based on published band assignment data (Bellamy 1975, pp. 5–9; Shearer 1989, pp. 376–379).

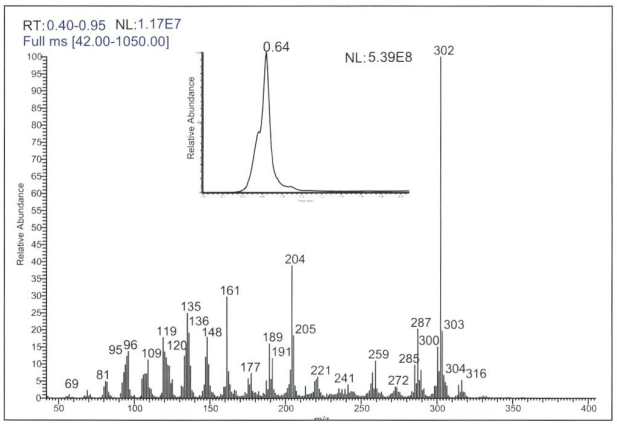

Fig. 25 DTMS spectrum of 'copaiva balsam'.

Basic lead white pigment

The FTIR spectrum of hydrocerussite or basic lead carbonate has been published by White (1974). The reference material analysed here (Fig. 26, Table 15) belongs to the SIK-ISEA pigment reference collection; no information is available as to its date of manufacture. The total ion chromatogram of basic lead carbonate (Fig. 27, Table 16) has two main events. The first event at 0.81 minutes (spectrum not shown) is dominated by one ion m/z 44 amu (CO_2) which corresponds to the decarboxylation of the pigment. The second event is shown in the spectrum. Isotopic finger-printing of lead allows for the ion attribution of the different clusters.

m/z	attribution	m/z	attribution	m/z	attribution
119	sesquiterpene	189	sesquiterpene	287	diterpenoid
135	diterpenoid abietane	204	sesquiterpene	300	diterpenoid
136	diterpenoid abietane	239	diterpenoid abietane	302	diterpenoid
148	sesquiterpene	259	diterpenoid abietane	314	diterpenoid
161	sesquiterpene	285	diterpenoid abietane	316	diterpenoid

Table 14 Assignments of the most intense peaks of the DTMS spectrum in Fig. 25.

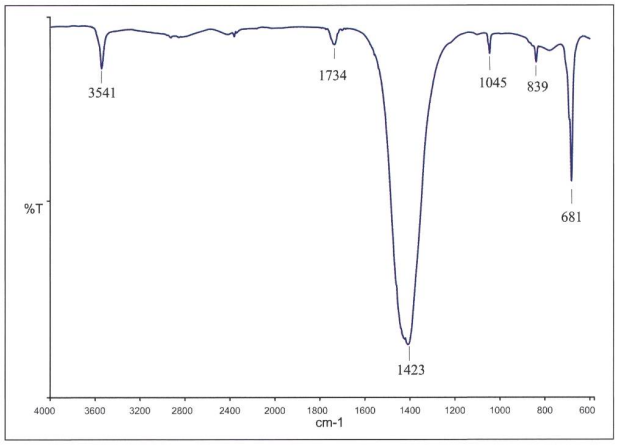

Fig. 26 FTIR spectrum of basic lead white pigment.

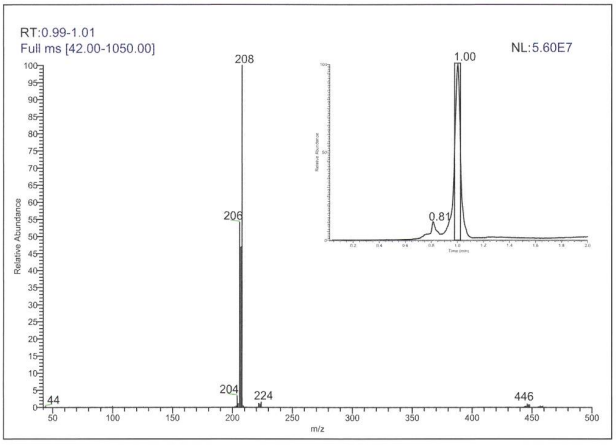

Fig. 27 DTMS spectrum of basic lead white pigment.

FTIR band cm^{-1}	functional group
3541	**O–H stretching**
1734	**C=O stretching (carbonate)**
1423	**ν_3 asymmetric stretching (CO_3^{2-})**
1045	**O-H deformation**
839	**ν_2 out-of-plane bending (CO_3^{2-})**
681	**ν_4 in-plane bending (CO_3^{2-})**

Table 15 Assignments of FTIR bands in Fig. 26.

m/z	attribution	m/z	attribution	m/z	attribution
44	$^{12}CO_2$	220	^{204}PbO	445	$^{206}Pb\ ^{207}PbO_2$
204	^{204}Pb	222	^{206}PbO	446	$^{206}Pb\ ^{208}PbO_2$
					$^{207}Pb\ ^{207}PbO_2$
206	^{206}Pb	223	^{207}PbO	447	$^{207}Pb\ ^{208}PbO_2$
207	^{207}Pb	224	^{208}PbO	448	$^{208}Pb\ ^{208}PbO_2$
208	^{208}Pb	444	$^{206}Pb\ ^{206}PbO_2$		
			$^{204}Pb\ ^{208}PbO_2$		

Table 16 Assignments of the most intense peaks of the DTMS spectrum in Fig. 27.

1 The three-digit, non-consecutive numbering of the tempera binders suggests that Urban tested hundreds of formulations, and rated only 13 as successful. The compilation found in Amiet's estate was probably copied by Amiet himself after Urban's (equally handwritten) original or, even more likely, after another copy thereof. For more details see Beltinger *et al.* 2015, pp. 58–71.

2 The paint was reconstructed in three different colours using the pigments cadmium orange, synthetic ultramarine and lead white, all important pigments identified in the palette used by Cuno Amiet in his early period. In this contribution however, we focus on the reconstructed lead white paint only as it is the most relevant for providing a direct comparison with the sample collected from Amiet's work *Hügel*.